General Disclaimer

One or more of the Following Statements may affect this Document

- This document has been reproduced from the best copy furnished by the organizational source. It is being released in the interest of making available as much information as possible.

- This document may contain data, which exceeds the sheet parameters. It was furnished in this condition by the organizational source and is the best copy available.

- This document may contain tone-on-tone or color graphs, charts and/or pictures, which have been reproduced in black and white.

- This document is paginated as submitted by the original source.

- Portions of this document are not fully legible due to the historical nature of some of the material. However, it is the best reproduction available from the original submission.

NASA

Technical Memorandum **79545**

Analysis of the Dynamics of Shifting Cultivation in the Tropical Forests of Northern Thailand Using Landscape Modeling and Classification of Landsat Imagery

Kaew Nualchawee and Craig Tom

MAY 1978

National Aeronautics and Space Administration

Goddard Space Flight Center
Greenbelt, Maryland 20771

Analysis of the Dynamics of Shifting Cultivation in the Tropical Forests of Northern Thailand Using Landscape Modeling and Classification of LANDSAT Imagery

Lee D. Miller
Senior Research Associate
Earth Res. Branch, NASA/GSFC
Greenbelt, MD 20771

Kaew Nualchawee
Department of Civil Engineering
Colorado State University
Ft. Collins, CO 80523

Craig Tom
HRB-Singer, Inc.
Ft. Collins, CO 80521

ABSTRACT

Landscape modeling is the process of overlay and analysis of a large number of multiple spatial variables extracted from maps, airphotos, LANDSAT imagery and other remotely sensed data. Its application to this problem has employed a data base containing 103 spatially registered variables. These variables have been assembled to model a site of 292.2 square kilometers at a 1 hectare resolution in the tropical forests of Northern Thailand which are subjected to the dynamic practice of shifting cultivation. Recent changes in land cover measured with 4 dates of sequential airphoto interpretation maps were used to model the overall trends and spatial trends in 6 forest and 3 agricultural land cover types occurring in the forest area. Computer comparison of the changes in 5 consecutive anniversary date LANDSAT images for 1972 through 1977 was completed with this data base to determine the usefulness of this simple image analysis approach for monitoring the dynamic changes in this forest cover. LANDSAT image classification was also tested within the context of the landscape model to determine the contribution of spatial overlays of ancillary data to final map classification accuracy for the 9 land covers. Topographic overlays were evaluated (slope, aspect, elevation, and distance to drainage) as well as cultural feature overlays (distance to roads and trails, permanent housing, and temporary huts). Stepwise discriminant analysis was employed as the classifier with 3 types of training sets (rectangular, aspect, and grid sampled training sets). Two assumptions of the apriori probabilities of occurrence of the 9 land covers within the site were also tested with this classifier, i.e., equal apriori probability of occurrence and probabilities proportional to the known occurrence of each cover type.

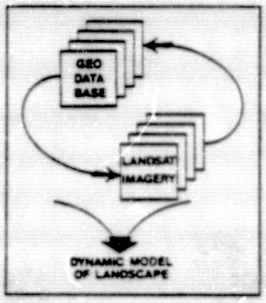

INTRODUCTION TO LANDSCAPE MODELING CONCEPT

What is Landscape Modeling?

Geographic data base and remote sensing technologies are about to be combined into a whole whose sum is greater than its parts. This serendipitous meeting of the separate technologies will provide a realistic, dynamic information base and associated analysis techniques for practical, environmentally oriented land planning. Landscape modeling is the name proposed for this fruitful combination, which organizes and overlays data from existing maps, analysis of remote sensing imagery, and tabular data into a single computer framework. This assemblage provides a multivariate, multitemporal mathematical model which represents the landscape much as a topographic map represents a three-dimensional model of the physical land surface. Coupled with this composite of data overlays is a collection of computer techniques which allow meaningful simulation of the spatial or map-like behavior of this landscape to natural and man-induced alteration and control. The current thrust of landscape modeling is the projection and display in a map form of the future landscape which would result from the continuation of current land management practices or the lack thereof. Success in this short-run objective has enabled the design of the computer techniques needed to predict various scenarios of anticipated landscape alternatives[1]. The scenarios evaluated could include diverse objectives, such as new forest management practices, new zoning patterns for urban land planning, alternate sites for a new power plant, or the impact of siting a new dam. Land management should be substantially improved if the future spatial implications of a contemplated action were modeled before any commitment to a fixed course of action.

How Does Landscape Modeling Relate to Remote Sensing?

Computer analysis of remote sensing imagery is symbiotic with the process of landscape modeling. It provides the important current and past land cover inputs to the landscape model. Detailed interpretation of low- and high-altitude airphotos acquired on various dates initially provided the maps used as quantitative measures of land cover change. LANDSAT remote sensing imagery, which has been continuously obtained since 1972, currently provides additional information of land cover change. Accurate computer analysis of land cover with LANDSAT imagery of various dates provides a more economical, timely, and direct measure of land change for land-

scape models and their projections of future land cover patterns.

The accuracy of the computer interpretation of the remote sensing imagery is, in turn, substantially improved by including a variety of landscape variables, such as slope and elevation. Thus, combining the available remote sensing imagery together with map information in the landscape model provides a basis for substantial improvements in both activities. Coincident, spatially registered overlays of readily available map information upon the multispectral imagery of LANDSAT have provided a basis for marked improvement in the accuracy of their computer interpretation to provide current land cover maps. These improved, automatically interpreted maps are of direct use in environmental planning. They also "feedback" directly into the landscape model to provide a timely measurement of past and present dynamic tendencies for change in land cover.

The bulk of this report will be devoted to the LANDSAT image analysis aspects of landscape modeling. A detailed discussion of land cover modeling has been reported elsewhere[2,3,4]. However, an overview of its application to this site will provide insight into the dynamics of tropical forest cover in areas of shifting cultivation. These dynamics must be dealt with in any meaningful remote sensing analyses.

BACKGROUND OF THE FOREST LANDSCAPE MODEL

Background of the Site Selection.

The landscape modeling efforts described in this report have been underway for approximately 6 years. The initial and more complex application of the approach has been a model of the evolution of natural lands to urban lands in the Denver metropolitan area of Colorado[5]. At the initiation of that study it was ascertained that a parallel application of the approach would be made to examine the evolution of forest land to temporary and permanent agricultural land. This application was thought, at that time, to provide a cleaner test of the concept, as fewer land cover types were involved* and one overall political control existed for the area rather than the more complex spatial political constraints of U.S. urban areas**. Man-made changes do dominate the forest area selected but are more closely coupled with the landscape. For example, the clearing of trees for shifting cultivation is known to be a function of land slope, soil type, and other landscape variables.

At first appraisal it might appear that such a project could be handicapped by a shortage of maps, airphotos and LANDSAT imagery. However, there was no shortage in the quantity of the data available, as the particular site has been and is being closely studied by various international and Thai agencies. Several key limitations did emerge as the study progressed and have impacted upon the approach and results.

- Inaccessibility prevented careful field control of the land cover maps derived by airphoto interpretation.
- No detailed soils map existed for the site although this is typical of tropical forest areas and must be compensated for by any procedures which are to be generalized.
- Excellent anniversary LANDSAT imagery exists for every year to date due to an annual cloud-free dry season. Unfortunately, this period has been too short to allow the collection of meaningful multiseasonal LANDSAT imagery; however, this is also typical of tropical forested areas.

Site Description.

This tropical forest site was selected to represent the northern region of Thailand. It is situated near the Golden Triangle at the corner intersection of China, Burma, Laos, and Thailand (Fig. 1). It represents mountainous area which was originally heavily forested but has been rapidly cleared for shifting cultivation of opium, dry-land rice, tea, and other cash crops. It is typical of a large portion of the world's tropical forests where cut-and-burn agriculture is out of balance with regrowth and the mountain slopes and watersheds are being rapidly denuded.

Construction of the Landscape Model.

The forest area modeled was enclosed in a rectangle of 432 square kilometers (24 km E-W and 18 km N-S) which was cellularized with a resolution of one hectare (approximately 2.5 acres) yielding 43,200 cells. The closed, irregularly bounded study site within this rectangle was limited to the area common to several of the special maps made available from the earlier analyses of the site by others. It consisted of an area of 292.9 km^2 or 29,290 square cells of 1 ha resolution and is an anti-watershed bounded by major water courses or drainages on all

* Nine forest/agricultural land cover types described the Thailand site, while 24 were required in the Denver site.

** The Denver site is approximately the same size but is made up of portions of 5 different counties which control the land use and thereby the land cover by using 5 different independent sets of zoning regulations.

sides with a mountain ridge in the center. The landscape model of this site consists to date of 103 image and map variables overlaid such that each constitutes a cellular data plane of 1 ha resolution covering at least the common area of 29,290 ha (Fig. 2). Utmost care has been exerted to insure that each of these data planes registers upon all others to the nearest 1 ha resolution cell[3]. Input of those data planes derived from existing maps and airphotos was completed entirely by a manual dot sample method[6]*. Area planes, such as topographic elevation and geology, are directly sampled cell-by-cell from 1:50,000 scale maps. Additional derived area planes are computed, such as topographic slope and aspect from elevation[7]. Point feature planes, such as the location of temporary huts or permanent dwellings, were interpreted for 4 different dates from low altitude, black-and-white airphotos[3]. These planes were then computed into minimum distance area planes[4]. Linear features, such as drainage and roads and trails, were similarly interpreted from the airphotos for 4 dates[3]. They were also converted by computation into minimum distance area planes[4]. Airphoto interpretation maps were prepared for 4 different dates for 9 forest and agricultural land cover types and overlaid onto the model via the area dot sampling procedure[3]. These 4 land cover maps were all interpreted by a single individual in a consistent fashion.

MODELING CHANGES IN FOREST LAND COVER

Visual Display of the Changes in Land Cover.

The 9 types of land cover interpreted on each of the 4 dates of airphotos (Figs. 3, 4, 5, and 6) include the 6 forest types of:

- dry dipterocarp forest
- mixed deciduous forest with teak
- dry evergreen forest
- dry dipterocarp forest with pine
- hill evergreen forest
- teak plantations

together with 3 agricultural land covers of:

- shifting cultivation
- irrigated rice paddies
- tea plantations.

Intercomparison of these land cover data planes of the site on a cell-by-cell basis yields graymaps of change which provide qualitative insight into the current imbalance between forest depletion by shifting cultivation (Fig. 7) and forest regeneration upon agricultural abandonment (Fig. 8). A tabulation of the amount of each land cover for each available date illustrates the rapid recent change in the use of this area (Fig. 9). Clearly the nominal 20 year cycle from forest to shifting cultivation and back to forest has been markedly shortened. A subsistence level, dry land, permanent agriculture is setting in with attendant deleterious environmental effects, such as the alteration of the basic hydrologic processes. Erosion of the soil is rapidly increasing with marked increase in sediment and water yield accompanied by shorter duration hydrographs. Thus the cut-and-burn process is rapidly approaching the irreversible point where all significant natural forest regeneration will permanently cease.

Trend Modeling of the Land Cover.

The assumption that future changes in land cover can be measured in terms of those which occurred in the recent past allows a simple projection of land cover of the area represented by a landscape model[5]. Cross-tabulation of each pair of consecutive land cover data planes in the landscape model (e.g., 1968 with 1972) provides a probability transition matrix. This matrix is applied in a Markov process to the distribution of land cover recorded in the second or more recent land cover data plane to project future trends**. Only a few years of validity may be assumed for these projections, as the processes controlling the land cover during the training period (i.e., 1968 to 1972) can only be assumed to persist for a few years into the future (i.e., >1972). The particular land cover trends based upon the most recent pair of land use planes in this landscape model predict that irrigated rice lands will continue to increase in the future as they did during the recent past or training period. However, this cannot be the case as the area of land suitable for irrigation is being rapidly exhausted even though it was not yet in short supply during the training period. This longer term breakdown of the Markov trend model points out that it has used only the actual changes in the recent land covers to project future trends. However, additional landscape parameters are available in the landscape model to improve the land cover modeling procedures.

Spatial Modeling of the Land Cover.

A much more complex model has been developed which is capable of projecting the future spatial behavior of the land cover of the site based upon controlling landscape features. Essentially, it takes all the specific changes in land cover tabulated between the two consecutive land cover data planes, groups them together into like changes, and correlates their

* Technical details on the construction of the data planes whose specific use is reported herein occurs as part of the caption for the figures illustrating those data planes and in the references noted. Illustrations of the data planes (Figs. 3 through 38) have been reproduced at a very small size in order to include the maximum amount of material in the limited pages allowed.

** Land cover trend models have been computed for the following pairs of dates: 1954 with 1972, 1954 with 1966, 1966 with 1968, and 1968 with 1972[3].

occurrence with the corresponding landscape parameters in the landscape model (e.g., slope, distance to roads and trails, etc.) using a multivariate approach. Exactly the same computational approach is taken as in the application of stepwise discriminant analysis to image classification except the class to be predicted is a specific change in land cover rather than a particular land cover. The variables used in this new type of classification are restricted to landscape parameters and no image parameters are included. The needed computational procedures have been worked out and spatial map projections of future land cover have been completed although they are not included here for the sake of brevity[5]. It is contemplated that the cell-by-cell overlay of these spatial model results onto the LANDSAT images already in the landscape model will provide a basis for improved image classification. Apriori knowledge (i.e., probability) of the land cover occurring in each individual image cell based on such spatial projections using earlier known land covers and landscape parameters should improve the single cell classification accuracy. Correspondingly, apriori knowledge of the overall land cover composition of the site will be subsequently shown to improve overall classification accuracy.

LANDSAT DIFFERENCING FOR FOREST LAND COVER CHANGE MAPS

The simplest LANDSAT image analysis undertaken was the cell-by-cell subtraction of each MSS band of one image from those of another anniversary image. The radiance differences which result range ± about zero and the ± magnitude of these differences correlate with various changes in land cover between the two images. For example, clearing the forest or brush cover to expose the soil and dead ground litter for shifting cultivation will increase the radiance in MSS-5 and decrease it in MSS-7, causing image differences greater than zero and less than zero, respectively*. Anniversary date image differencing and ratioing has not yet been widely tested due to the difficulties and costs associated with the rectification of several LANDSAT scenes to a common cellular base. The supplying of already rectified imagery from LANDSAT 3 by NASA/GSFC and the EROS Data Center should increase the interest in these procedures and their testing. Ground truth collection for the identification of the changes detected is also more complicated as it must be performed twice.

Application of LANDSAT image differencing to map changes in tropical forest cover was tested on this site since an understanding of its dynamics was available. The site is also small so that independent geometric rectification was feasible for each LANDSAT anniversary image of 1973, 1974, 1975, 1976, and 1977. The 4 MSS bands representing each of these images were first transformed to remove the major sensor distortions and resampled into the 1 ha square cell data planes using a nearest neighbor algorithm[9]. This new cell is approximately 2 times the area of the original LANDSAT picture element and thus about 50% of the LANDSAT elements were transferred to this new format (Figs. 11 and 12). The topographic and other landscape maps introduced into the landscape model were accurate only to the 1 ha cell size and the LANDSAT imagery was undersampled to match these data planes. This undersampling procedure has not appeared to introduce any noticeable effects on any of the LANDSAT image processing activities except the incorporation of some single cell noise into the difference graymaps where the 2 independent rectifications do not sample precisely the same nearest neighbor. The effect of most of this noise was removed by the application of a low band pass spatial filter to each difference image before its display as a graymap[5].

Little experience with image differencing can be found in the literature in connection with tropical forests and shifting cultivation. Thus the initial question addressed was what time base should be used between images (e.g., 1 year, 2 years, etc.). Subsequently, all combinations were computed and 1 year intervals found to produce the most consistent results. The image difference data planes have a narrow histogram of Gaussian appearance in all cases if the solar angle differences between the 2 dates is no more than a few degrees. Location of the data ranges to either side of the mean which contain the land cover changes sought is not straightforward unless accurate ground control is available for both image dates. The histogram of the whole image difference data plane for a given MSS band reverses from positive to negative if the order of subtraction of the two images is reversed. This is the same as changing the arithmetic sign of the solar angle difference. However, this arithmetic sign can also be changed by a small change of 1 or 2 weeks in the exact calendar date of one of the images selected to represent the "anniversary" dates. This also causes a positive to negative reverse of the histogram of this data plane. Considerable additional experience with this simple procedure is still needed to obtain a more generalized understanding of its application to monitoring forest cover type and change. For example, increasing the solar angle difference between the two images used enhances the contrast of one forest type relative to another in the difference image. This might be due to the inherent differences in the tree stand morphology

---

* The mean values of these difference data planes can fluctuate several units either way from zero due to overall image differences between the two anniversary dates such as those induced by different atmospheric absorption in one image versus the other.

of the 2 forest types which cause different subtle shadow effects in the images selected, thus allowing discrimination of these types in the difference graymap.

Consistent detection of the area of shifting cultivation was observed for each of the graymaps produced to display the 1 year anniversary difference images of MSS-7 (Figs. 13, 14, 15, and 16). The first two or earlier date difference graymaps emphasize the general pattern of shifting cultivation (Figs. 13 and 14). The remaining two more recent graymaps (Figs. 15 and 16) emphasize the active areas of shifting cultivation at the highest altitudes at the center of the site which have been cleared and planted to opium poppies during the intervals between images. The relative detection of old versus active shifting cultivation in this sequence of 4 consecutive 1 year interval difference graymaps is not clearly understood although it is due in part to the narrowness of the histograms noted earlier which markedly restricts the exact selection of the difference data ranges to be displayed in the graymap.

Consistent patterns of the movement of permanent agriculture into the forested portion of the site can be detected annually in the MSS-5 image difference graymaps (Figs. 17, 18, 19, and 20). Unfortunately, these changes can be confused with radiance differences in the areas of agriculture present on both dates where changes in crop type or planting date occur from year to year*. However, careful analysis of the original airphoto land cover maps shows a steady progression of permanent agriculture into the forest from the NE and SE corners[3]. This steady encroachment of irrigated and dry land rice, together with orchards, can readily be detected on the difference graymaps.

Image differencing also tends to compensate in part for topographic induced radiance variation if the solar angle difference between the images is not too large. More meaningful compensation for these topographic effects would result if the cell-to-cell image difference were weighted by the radiance value of each cell for one of the input images. This "automatic gain control" would adjust the image differences for similar land cover changes in the shadows or sunlit areas to the same numeric value.

LANDSAT FOREST LAND COVER CLASSIFICATION WITH ANCILLARY DATA

Classification with Topographic Overlays.

LANDSAT classification in areas of significant relief is limited in accuracy by that portion of the radiance variation created by the terrain which is independent of the surface cover type. Deep shadows represent the limiting condition but surface areas which are not in shadows but merely at different topographic slopes and aspects can exhibit significant topographic induced radiance variation within a specific land cover type. A large portion of the economically important forested areas of the world occur in areas of moderate to severe relief and these are also the areas of least knowledge of the forest type, condition, and productivity. The forest site selected for this analysis is typical of the rugged tropical forest remaining in Thailand and adjacent Asian nations. It is the very ruggedness of the terrain which has preserved a portion of these natural forests to the present time. A quick comparison of the rectified 1973 LANDSAT images (Figs. 11 and 12) with the 1972 land cover clearly illustrates that the radiance distributions imaged by LANDSAT are dominated by topographic effects and show little resemblance to the land cover (Fig. 6)**. The procedures developed for the application of LANDSAT classification methods to such areas must cope with these terrain induced variations. Three different attacks on this problem have been initiated as follows:

- Selection of training sets to represent each cover type as more than one class according to its slope and aspect range.
- The overlay of topographic features as data planes onto the imagery and their incorporation as input variables in the classification.
- A deterministic adjustment or preprocessing of the LANDSAT MSS bands to remove the major portion of the topographic induced variation.

The results of the first two approaches are reviewed while the third has not yet been successfully completed although a graymap of the site very similar in appearance to that of MSS-7 (Fig. 12) has been simulated. This computation of the radiance variation in MSS-7 uses the topographic slope and aspect data planes and other data to compute a new data plane consisting of the cell-by-cell near-instantaneous solar insolation at the exact time of the LANDSAT image[4].

The topographic overlays employed in the two empirical approaches to terrain compensation were derived from the 1:50,000 topographic map of the site. The elevation was sampled for each of the 29,290, 1 ha cells yielding the initial data plane (Fig. 21). This cell by cell deter-

* This is not necessarily an undesirable condition, but one we do not understand how to sort out and use to advantage.

** Note that the December airphotos used in preparing the 1972 land cover map are separated by about 1 month from the 27 January 1973 LANDSAT image and thus represent the same year and dry season.

mination was very tedious but yielded the most accurate elevation data plane of any technique available*. The slope (Fig. 22) and aspect (Fig. 23) data planes were obtained by fitting a faceted surface to the elevation data plane and computing the slope and aspect of this surface at each of the 29,290 cells. The drainage map was interpreted from the 1972 airphotos and converted to a binary data plane. Each remaining cell not occupied by a drainage element was assigned a value equal to the number of cell units (i.e., distance) to the nearest cell occupied by the drainage in a N-S and/or E-W excursion (Fig. 24). These 4 topographic data planes were overlaid in a cell-by-cell fashion onto the 4 MSS bands and 6 ratios of MSS bands in the landscape model.

Stepwise discriminant analysis was employed as the classifier in these analyses as it is reasonably forgiving of the non-Gaussian nature of the data to be classified. Extensive training set classification with a wide variety of image and landscape variables and types of training sets was completed. This provided the basis for the selection of the training sets and variables to be tested for their final verification or map classification accuracy. These final verification results will be summarized here by the illustration of the actual classification maps and their verified accuracies. At this point it is appropriate to note that, based upon training set accuracies, it was determined that the 6 ratios of the 4 MSS bands contributed little to the classification accuracy and they were omitted from further analyses. The impact of three types of training sets tested will be presented and they are:

- RECTANGULAR TRAINING SETS consisting of several rectangular groups of cells selected to represent each of the 8 cover types** as identified on the 1972 land cover data plane.
- ASPECT TRAINING SETS where each of the 8 cover types identified on the 1972 land cover data plane, except irrigated rice, were subdivided into 2 new classes and represented by rectangular groups of cells consisting of the particular cover type on sun-facing and opposite-facing topographic aspects. This yielded 15 classes which were regrouped back into the 8 original classes after classification but before display or verification.
- GRID SAMPLED TRAINING SETS where every third row and column of cells in the 1972 land cover data plane were extracted and regrouped into 8 training sets representing the land covers.

Two assumptions for the apriori probabilities of occurrence of each land cover were tested as follows:

- EQUAL APRIORI PROBABILITY of occurrence of each cover type in the area to be mapped.
- PROPORTIONAL APRIORI PROBABILITY of occurrence of each cover type in the area mapped, where the probabilities were taken as directly proportional to the populations of each of the cover types in the grid sampled training sets.

The 3 training approaches, together with the 2 types of initial assumptions of apriori probability of the final map composition, yielded 8 classification maps with MSS bands 5 and 7 (Fig. 25), the 4 MSS bands (Fig. 26), and the 4 MSS bands with topographic variables (Figs. 27 through 32). Visual insight into the success of these approaches to mapping shifting cultivation can be directly observed from the classification maps. Overall performance of the classifiers tested is best evaluated by the cell-by-cell verification of all 29,290 cells in the 1972 land cover data plane to be subsequently explained and presented.

Classification with Cultural Feature Overlays.

The distribution of three types of cultural features was mapped from each set of airphotos and converted into a data plane, specifically, the location of permanent housing, temporary huts, and roads and trails (Fig. 33). Each of these 3 types of features was computed into minimum distance planes in a fashion similar to that of the drainage plane (Figs. 34, 35, and 36). These new data planes were overlaid upon the 4 MSS bands and 4 topographic variables to determine their additional contribution to the classification results***. Since there is a close correlation between the location of these cultural features and the surrounding land cover it seemed reasonable that they would further improve the classification maps (Fig. 37).

Verification of the Accuracy of the Classification Maps.

The overall performance of the various classifiers tested was directly evaluated since the

* Practical future applications might employ something like a cell-by-cell stereoscopic satellite capable of providing the synchronized elevation values needed for terrain compensation during land cover classification of multispectral imagery.

** The ninth cover type, representing teak plantations, occupied only 40 ha of the site and was omitted for these classifications.

*** This may appear to employ circuitous logic; in other words, that such cultural features are part of the desired solution and not part of the input data. However, we have been careful to use the words "land cover" whereas these cultural features represent "land use". They might well be quickly mapped as point and line features from airphotos or satellite side-looking radar and added to the LANDSAT classification procedure to assist it to "paint" in the detailed areas of land cover.

"answer" is already available for each of the 29,290 cells classified in the form of the 1972 land cover data plane. A cell-by-cell comparison of the particular classification map with the land cover map yielded a simple verification display where a cell can quickly be identified as right (black) or wrong (white) if its classification checks with the known land cover (Fig. 38). These verification displays are useful to quickly determine the overall results of the classification and determine if any spatial bias exists in the classifier. The percentage of each cover type correctly classified, together with the overall accuracy, directly compares the various approaches (Table 1).

It must be noted that the percentage of correctly mapped points in such a verification cannot be expected to closely approach 100%. The airphoto interpretation maps of land cover have their own inherent accuracy which is not 100%. This initially impacts on the training set identification with these land cover maps. The impact is even greater during the verification of the LANDSAT classification results with the "known" airphoto derived land cover maps. The verification accuracy can only asymptotically approach the accuracy of the airphoto land cover map with the inclusion of each additional variable or set of variables. For example, assume that the land cover map derived from the airphotos is 70% correct; that is, if 10 random cells were checked on the ground 7 of the 10 would have been assigned by the photo interpretation to the correct cover type*. The classification map may also be 70% correct relative to ground conditions. Thus, verification of the LANDSAT classification map against the airphoto map will produce a 70% x 70% or 49% verification accuracy. Where training sets have been identified from the same airphoto land cover map a tendency will exist to bias the classification solution toward the map results and away from the real ground conditions somewhat increasing this 49% figure.

The verified map classification achieved the best overall accuracy of 55.4% with the grid sampled training sets** and proportional probabilities. Examination of the results of this approach for each combination of variables computed illustrates that it does asymptotically approach the limit set by the accuracy of the ground "truth" in the form of the 1972 land cover map (Table 1). Independent tests of grid sampled training set against other training set approaches for the Denver metropolitan landscape model also produced similar superior results even though a larger number of classes were sought[2]. This grid sample approach does not produce as high a training set accuracy, as it has been deliberately designed to include all the spectral variability in the area to be mapped. Rectangular or other area type training sets perform best when training set accuracy is the criterion in that they have been deliberately selected to minimize spectral variability. Subsequent application of rectangular or areal training sets to the "real" world, i.e., the area to be mapped with all its spectral diversity, has demonstrated that high training set accuracies do not extend into higher map verification accuracies[2].

Training set accuracies achieved with grid sampled training sets are essentially equal to the final map verification accuracies since the grid training sets are selected to be representative of the total area to be mapped. This provides one additional important advantage not possessed by rectangular or areal training sets. Any optimization done upon grid sampled training sets will also optimize the map classification operations, for example, the selection of an optimal subset of spectral bands for computational economy from among a suite of multispectral-multiseason images. Optimization of these features based upon rectangular or areal training sets does not necessarily extend to the final map classification employing these training sets.

Obtaining grid or random single cell training sets may appear too tedious to be practical, but this is not the case. First, the sample need not be nearly so large a percentage of the area to be mapped as was the case in this research (i.e., 11.1%). Second, the approach increases the accuracy of the photo interpretation and reduces the human tedium and monetary cost of acquiring the training data. All the photo interpreter has to do is accurately identify the land cover at specific preselected points on individual airphotos or stereo pairs. There is no need for the error prone spatial generalization which is required in making maps or to a lesser extent in defining rectangular or irregularly shaped areal training sets.

---

* A reasonable assumption in this case, as seen from the large amount of spatial generalization which exists in the 4 airphoto land cover maps.

** The grid sampled training sets used here are equivalent to random samples taken from the same area if the sample sizes are sufficiently large. Using a grid is simply a convenient way to extract the samples from cellularized data.

REFERENCES

[1] Miller, L. D., C. Tom, and K. Nualchawee. 1977. Remote sensing inputs to landscape models which predict future spatial patterns for hydrologic models. U.N. Water Conference, Technical and Scientific Sessions on Water Resources, Mar del Plata, Argentina (also NASA/ Goddard Space Flight Center, Rep. X-923-77-115, Greenbelt, MD). 41p.

[2] Tom, C. and L. D. Miller. 1978. Spatial inventory and modeling of land use/ Denver metropolitan area, with inputs from maps, airphotos, and LANDSAT. NASA/Goddard Space Flight Center, Tech. Rep., Greenbelt, MD. 250p.

[3] Wacharakitti, S., L. D. Miller, and C. Tom. 1975. Tropical forest land use evolution/ twenty year landscape model with inputs from existing maps, historical airphotos and ERTS satellite imagery. Colorado State Univ., Environmental Engineering Tech. Rep. 1, Ft. Collins. 217p.

[4] Nualchawee, K., L. D. Miller, and C. Tom. 1978. Spatial inventory and modeling of land cover of Northern Thailand/ with inputs from maps, airphotos, and LANDSAT. NASA/Goddard Space Flight Center, Tech. Rep., Greenbelt, MD. 240p.

[5] Miller, L. D. 1973. Satellite monitoring of regional open space encroachment (Denver, Colorado). Colorado State Univ., Dept. Civil Engineering, Progress Rep. 1, Ft. Collins. 20p.

[6] Tom, C. H., L. D. Miller, S. Krebs, and R. Aukerman. 1974. The design of a model to project land uses and predict open space encroachment patterns/ Denver metropolitan area. Colorado State Univ., Final Rep./Bur. Outdoor Recreation Contract 3-14-07-03, Ft. Collins. 195p.

[7] Tom, C. H. 1975. Technical documentation for the Colorado State Forest Service "TOPOMAP" slope/aspect mapping system. Colorado State Univ., Land Use Planning Info. Rep. 4B, Ft. Collins. 23p.

[8] Sung, Q. C. and L. D. Miller. 1977. Land use/land cover mapping (1:25,000 of Taiwan, Republic of China by automated multispectral interpretation of LANDSAT imagery. NASA/Goddard Space Flight Center, Rep. X-923-77-210, Greenbelt, MD. 168p.

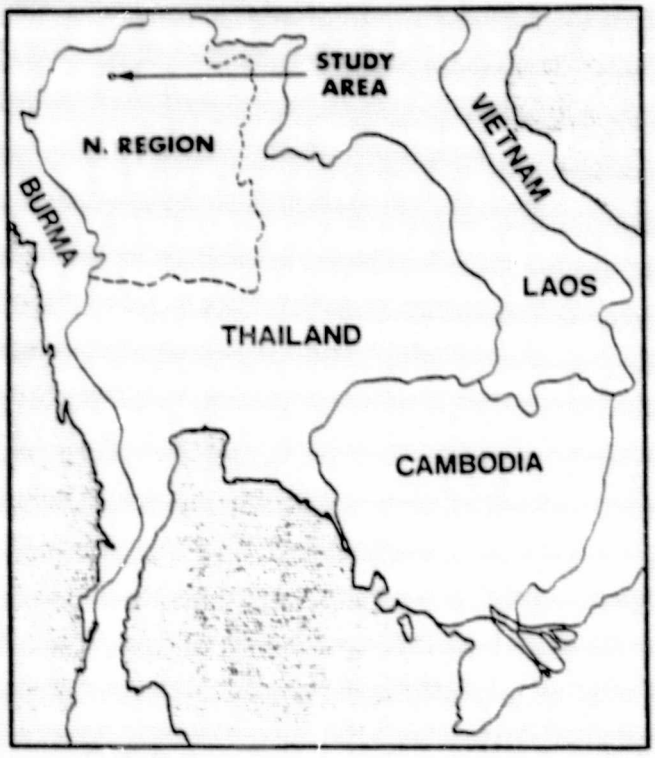

FIGURE 1. LOCATION OF THE STUDY SITE[3].

The irregular study site is 292 square kilometers in Northern Thailand near the area of the intersection of the China, Burma, Laos and Thailand borders called the Golden Triangle. It is representative of the general area which is mountainous and was originally heavily forested but has been rapidly cleared for shifting cultivation of opium, dry-land rice and other cash crops.

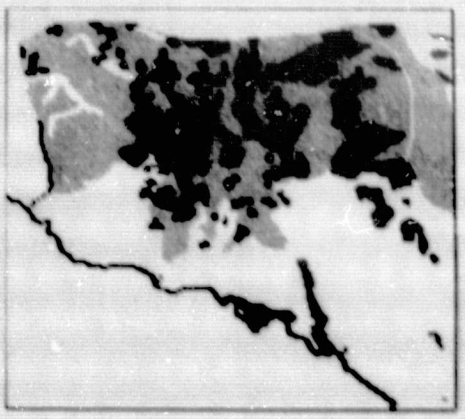

6 LAND USE SUBMODEL VARIABLES:
- 1954
- 1966
- 1968
- 1970
- 1972

→ Forest Types and Related Land Use

- Potential Natural Vegetation

10 CULTURAL FEATURES SUBMODEL VARIABLES:
- 1954
- 1966
- 1968
- 1970
- 1972

→ Minimum Distances to Temporary Structures

- 1954
- 1966
- 1968
- 1970
- 1972

→ Minimum Distances to Permanent Structures

5 TRANSPORTATION SUBMODEL VARIABLES:
- 1954
- 1966
- 1968
- 1970
- 1972

→ Minimum Distances to Roads and Trails

9 PHYSIOGRAPHIC SUBMODEL VARIABLES:
- Topographic Elevation
- Topographic Slope (2 versions)
- Topographic Aspect
- Drainage (2 versions)
- Geology (2 versions)
- LANDSAT Image Insolation

73 LANDSAT IMAGE VARIABLES:
- MSS-4 Visible Green
- MSS-5 Visible Red
- MSS-6 Solar Infrared
- MSS-7 Solar Infrared
- 6 MSS Channel Ratios
- 4 MSS Insolation Ratios

→ For 5 Anniversary Dates

- Photo Interpretation MSS-5
- Photo Interpretation MSS-7
- Photo Interpretation MSS Color IR

→ 1 Date Only

FIGURE 2. CONCEPTUALIZATION OF THE LANDSCAPE MODEL CONSTRUCTED FOR THE STUDY AREA[1].

Listed are the 103 variables which have been overlaid as individual data planes in the form of 29,290 square cells of 1 ha resolution. Each of these data planes contains 43,200 cells within the inscribing rectangular area but the information content is limited to the irregularly bounded area common to several of the special maps made available by other studies of the area This irregular site consists of an anti-watershed bounded by major watercourses or drainages on all sides with a mountain ridge in the center.

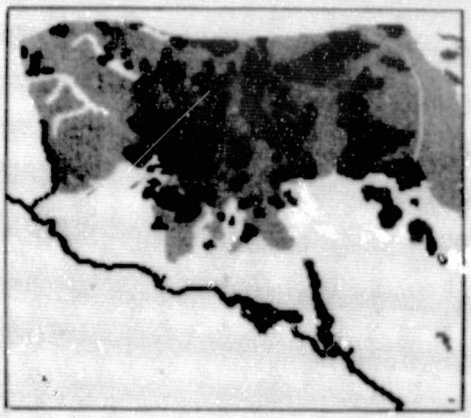

FIGURE 3. 1954 LAND COVER TYPE MAP[3].

black ——→ *shifting cultivation and tea*
medium gray ——→ *irrigated rice*
light gray ——→ *hill evergreen forest*
white ——→ *4 other forest types*

A land cover map was interpreted from 19 medium altitude 1:60,000 black and white air photos of Jan. 1954 and compiled at 1:50,000. The map was, in turn, digitized to record the spatial distribution of each of the 8 land cover types in the 1 ha cellular data plane format.

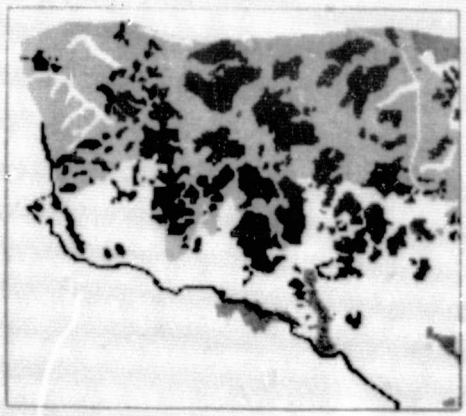

FIGURE 4. 1966 LAND COVER TYPE MAP[3].

black ——→ *shifting cultivation and tea*
medium gray ——→ *irrigated rice*
light gray ——→ *hill evergreen forest*
white ——→ *4 other forest types*

A land cover map was interpreted from 76 low altitude 1:20,000 black and white air photos of Jan. 1966 and compiled at 1:50,000. The map was, in turn, digitized to record the spatial distribution of each of the 8 land cover types in the 1 ha cellular data plane format.

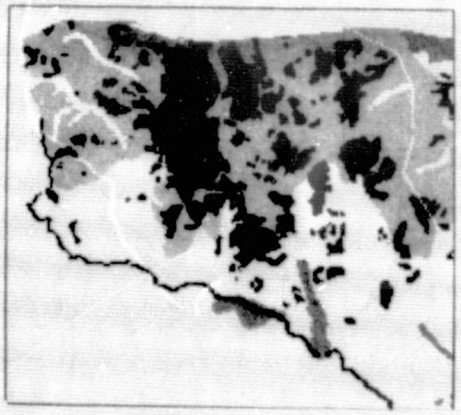

FIGURE 5. 1968 LAND COVER TYPE MAP[3].

black ——→ *shifting cultivation and tea*
medium gray ——→ *irrigated rice*
light gray ——→ *hill evergreen forest*
white ——→ *4 other forest types*

A land cover map was interpreted from 70 low altitude 1:25,000 black and white air photos of Jan. 1968 and compiled at 1:50,000. The map was, in turn, digitized to record the spatial distribution of each of the 8 land cover types in the 1 ha cellular data plane format.

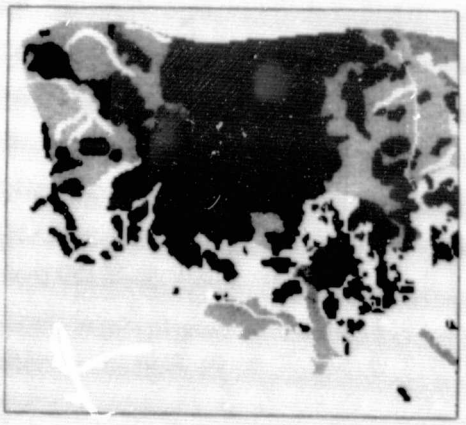

FIGURE 6. 1972 LAND COVER TYPE MAP[3].

black ——→ *shifting cultivation and tea*
medium gray ——→ *irrigated rice*
light gray ——→ *hill evergreen forest*
white ——→ *4 other forest types*

A land cover map was interpreted from 75 low altitude 1:20,000 black and white air photos of Dec. 1972 and compiled at 1:50,000. The map was, in turn, digitized to record the spatial distribution of each of the 8 land cover types in the 1 ha cellular data plane format.

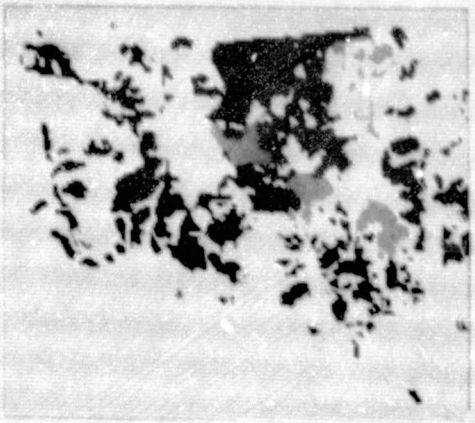

FIGURE 7. 1968 TO 1972 FOREST DEPLETION MAP[3].

black ——→ *forest converted to shifting cultivation*
dark gray ——→ *forest converted to tea plantations*
light gray ——→ *forest converted to irrigated rice paddies*

Obtained by a cell-by-cell comparison of the 1972 land cover (Fig. 6) with that of 1968 (Fig. 5).

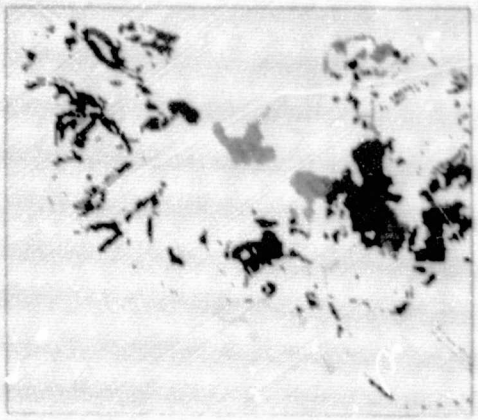

FIGURE 8. 1968 TO 1972 FOREST REGENERATION MAP[3].

black ——→ *abandoned land regrowing to forests*
dark gray ——→ *new tea plantations*
light gray ——→ *new irrigated rice paddies*

Obtained by a cell-by-cell comparison of the 1972 land cover (Fig. 6) with that of 1968 (Fig. 5).

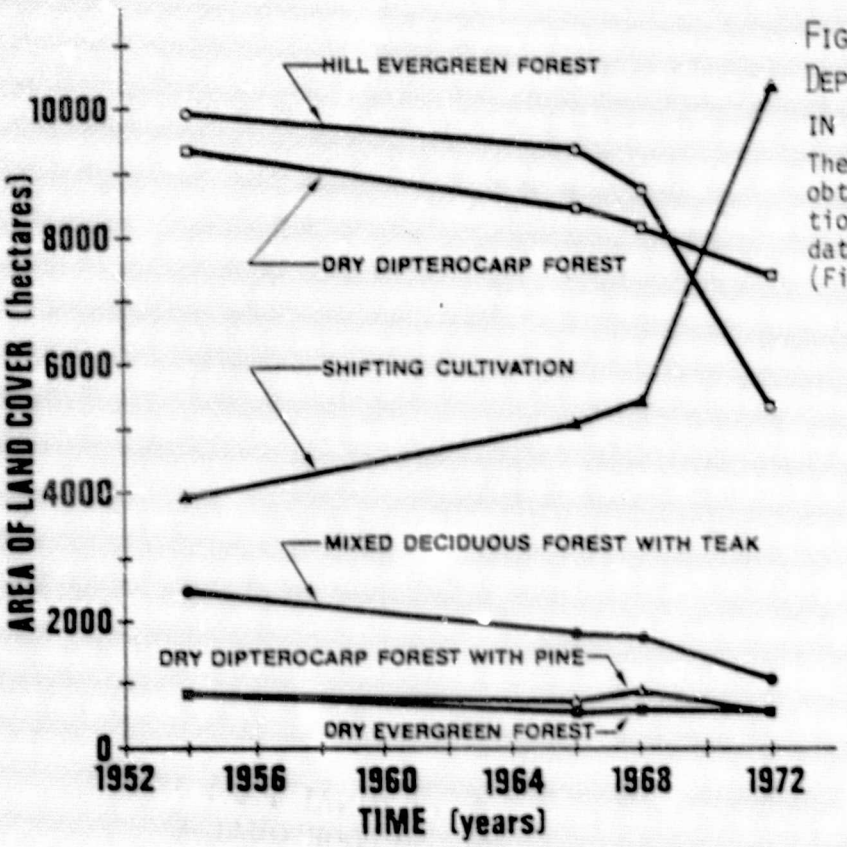

FIGURE 9. HISTORICAL FOREST COVER DEPLETION AND THE CONCOMITANT INCREASE IN THE AREA OF SHIFTING CULTIVATION.

The area of each land cover type was obtained by a simple computer tabulation of the 1 ha cellular land cover data planes for the dates available (Figs. 3, 4, 5, and 6).

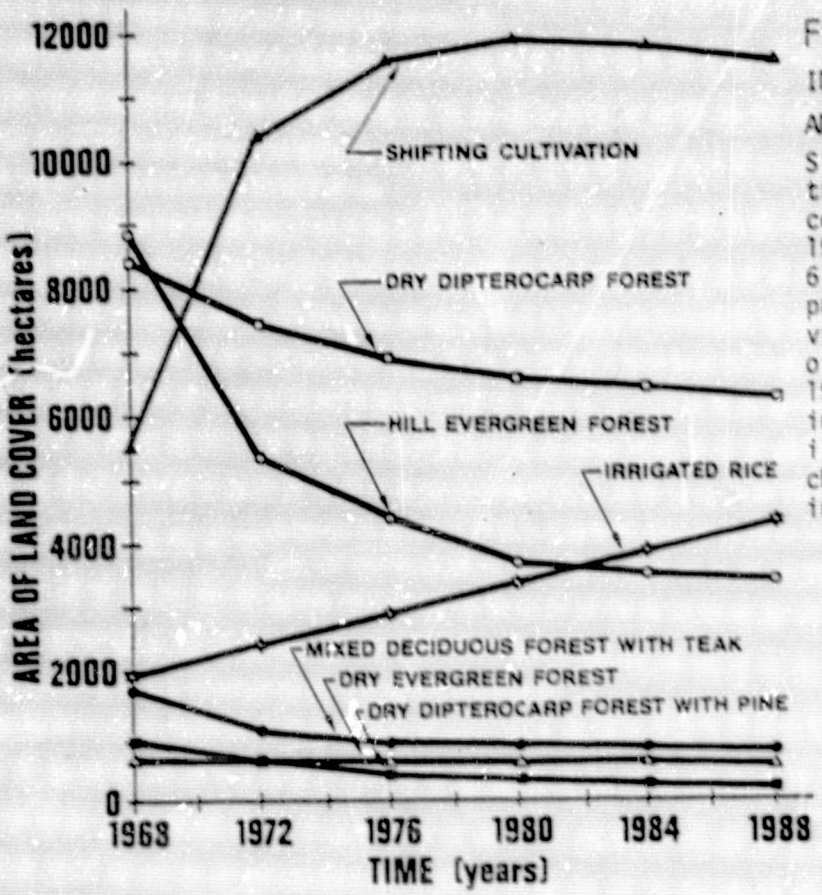

FIGURE 10. PREDICTIONS OF FUTURE TRENDS IN THE AMOUNT OF EACH FOREST COVER TYPE AND COMPETING AGRICULTURAL LAND USE[3].

Simulated using a Markov process and transition matrix provided by the 29,290 cell-to-cell comparisons of the 1968 to 1972 land cover data planes (Figs. 5 and 6). Similar simulations have been computed using the transition matrices provided by each of the consecutive pairs of dates of 1954 to 1966 and 1966 to 1968 as well as the longer overall time interval of 1954 to 1972. These models illustrate the tendencies for land cover changes in the study area due to evolving forest management policies.

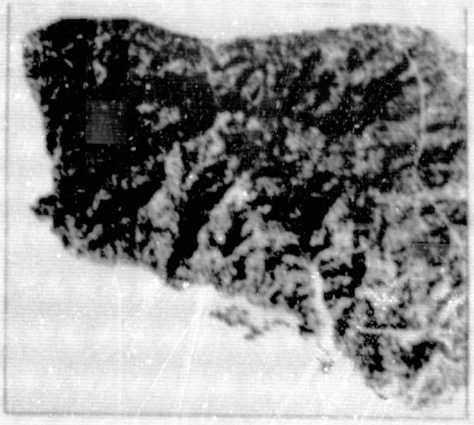

FIGURE 11. LANDSAT MSS-5 GRAYMAP[1].

(LOWEST RADIANCES IN BLACK)

This LANDSAT red (0.6 to 0.7 μm) image was taken 27 Jan. 1973 and has been rectified and resampled using a nearest neighbor algorithm to match the 1 ha cellular data plane format.

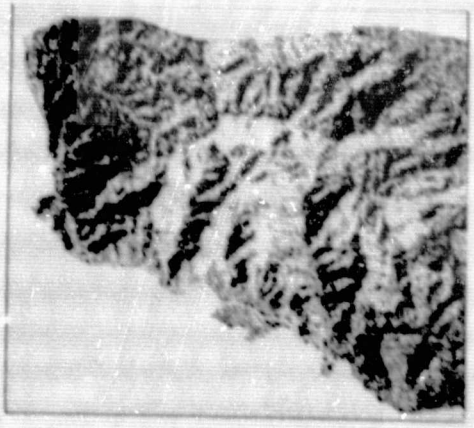

FIGURE 12. LANDSAT MSS-7 GRAYMAP[1].

(LOWEST RADIANCES IN BLACK)

This LANDSAT photo infrared (0.8 to 1.0 μm) image was taken 27 Jan. 1973 and has been rectified and resampled using a nearest neighbor algorithm to match the 1 ha cellular data plane format.

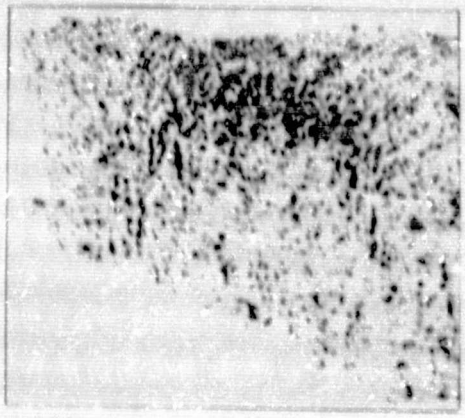

FIGURE 13. 1974-1973 LANDSAT MSS-7 DIFFERENCE GRAYMAP*.

(SMALLEST NEGATIVE RADIANCE DIFFERENCES IN BLACK)

The images were taken 22 Jan. 1974 and 27 Jan. 1973 yielding a solar angle difference of -1°. Each image was independently rectified and resampled with a nearest neighbor algorithm to match the 1 ha cellular data plane format. The 1973 image was subtracted from the 1974 image on a cell-by-cell basis. A low frequency spatial band pass filter was then applied to remove most of the single cell noise.

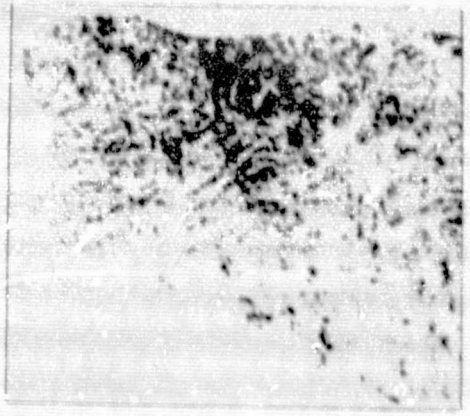

FIGURE 14. 1975-1974 LANDSAT MSS-7 DIFFERENCE GRAYMAP*.

(LARGEST POSITIVE RADIANCE DIFFERENCES IN BLACK)

The images were taken 13 Feb. 1975 and 22 Jan. 1974 yielding a solar angle difference of +1°. The difference image was computed just as in Figure 13 above.

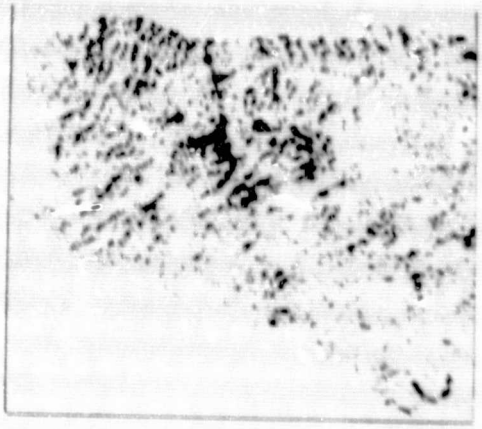

FIGURE 15. 1976-1975 LANDSAT MSS-7 DIFFERENCE GRAYMAP*.

(LARGEST POSITIVE RADIANCE DIFFERENCES IN BLACK)

The images were taken 26 Feb. 1976 and 13 Feb. 1975 yielding a solar angle difference of +3°. The difference image was computed just as in Figure 13 above.

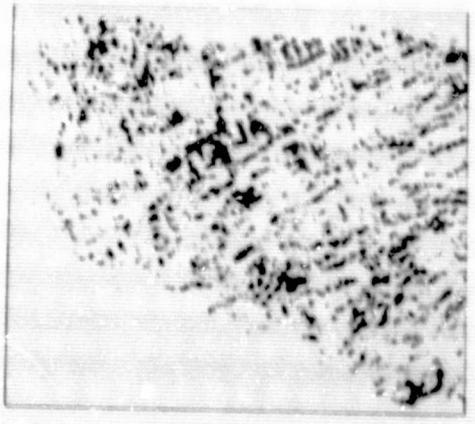

FIGURE 16. 1977-1976 LANDSAT MSS-7 DIFFERENCE GRAYMAP*.

(LARGEST POSITIVE RADIANCE DIFFERENCES IN BLACK)

The images were taken 2 Feb. 1977 and 26 Feb. 1976 yielding a solar angle difference of -7°. The difference image was computed just as in Figure 13 above.

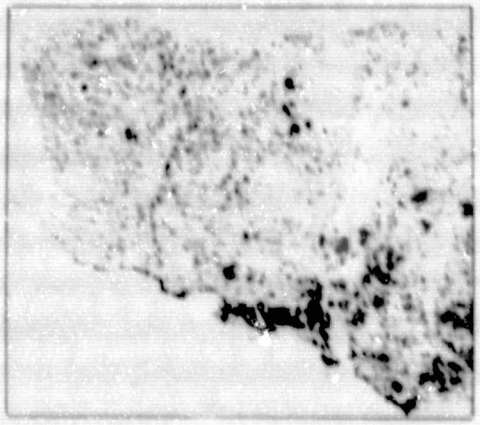

FIGURE 17. 1974-1973 LANDSAT MSS-5 DIFFERENCE GRAYMAP*.

(LARGEST POSITIVE RADIANCE DIFFERENCES IN BLACK)

The images were taken 22 Jan. 1974 and 27 Jan. 1973 yielding a solar angle difference of -1°. Each image was independently rectified and resampled with a nearest neighbor algorithm to match the 1 ha cellular data plane format. The 1973 image was subtracted from the 1974 image on a cell-by-cell basis. A low frequency spatial band pass filter was then applied to remove most of the single cell noise.

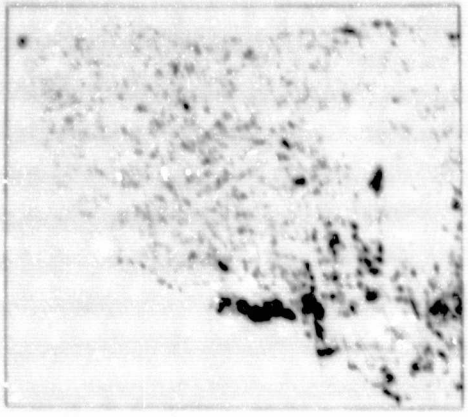

FIGURE 18. 1975-1974 LANDSAT MSS-5 DIFFERENCE GRAYMAP*.

(SMALLEST NEGATIVE RADIANCE DIFFERENCES IN BLACK)

The images were taken 13 Feb. 1975 and 22 Jan. 1974 yielding a solar angle difference of +1°. The difference image was computed just as in Figure 17 above.

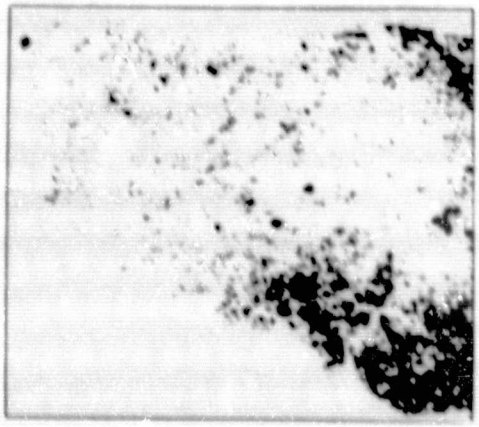

FIGURE 19. 1976-1975 LANDSAT MSS-5 DIFFERENCE GRAYMAP*.

(SMALLEST NEGATIVE RADIANCE DIFFERENCES IN BLACK)

The images were taken 26 Feb. 1976 and 13 Feb. 1975 yielding a solar angle difference of +3°. The difference image was computed just as in Figure 17 above.

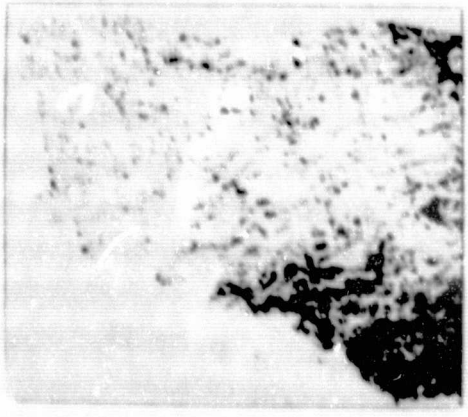

FIGURE 20. 1977-1976 LANDSAT MSS-5 DIFFERENCE GRAYMAP*.

(SMALLEST NEGATIVE RADIANCE DIFFERENCES IN BLACK)

The images were taken 2 Feb. 1977 and 26 Feb. 1976 yielding a solar angle difference of -7°. The difference image was computed just as in Figure 17 above.

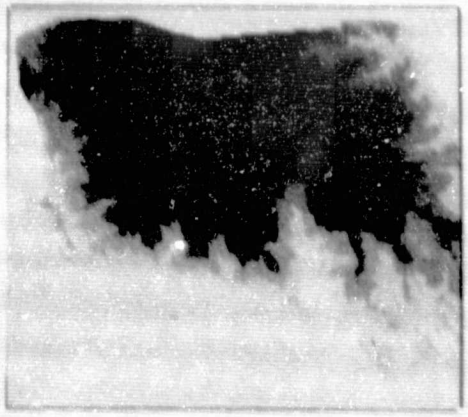

FIGURE 21. TOPOGRAPHIC ELEVATION MAP[3].

(HIGHEST ELEVATIONS IN BLACK)

The elevation of each individual 1 ha cell was estimated to within 10 meters from a 1:50,000 scale topographic map for each of the 29,290 cells using a dot grid overlay. The contour interval between gray steps of the display is 304 m (1,000 ft).

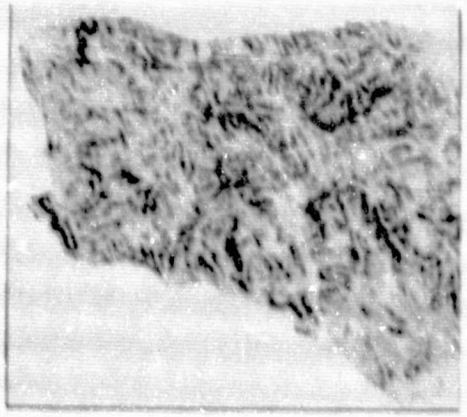

FIGURE 22. TOPOGRAPHIC SLOPE MAP[3].

(STEEPEST SLOPES IN BLACK)

The slope of each individual 1 ha cell was computed by fitting a regression least-square plane to the topographic elevations of a 3 by 3 array of cells and determining the slope of that surface to the nearest 0.1% and assigning it to the center cell of the array. Repeating the process over the whole elevation plane provides this slope data plane.

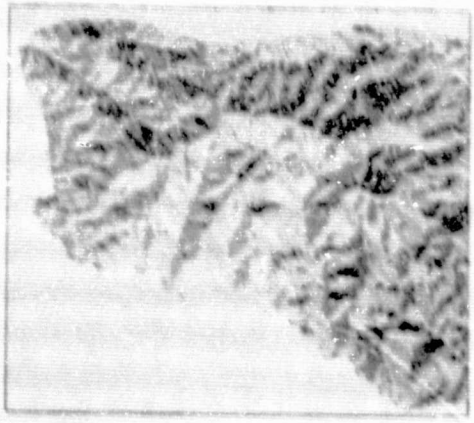

FIGURE 23. TOPOGRAPHIC ASPECT MAP[3].

(NORTH-ORIENTED AREAS IN BLACK)

The aspect of each individual 1 ha cell was computed by fitting a regression least-square plane to the topographic elevations of a 3 by 3 array of cells and determining the aspect (i.e., compass direction of the perpendicular to the plane) of that surface to the nearest 1° and assigning it to the center cell of the array. Repeating the process over the whole elevation plane provides this aspect data plane.

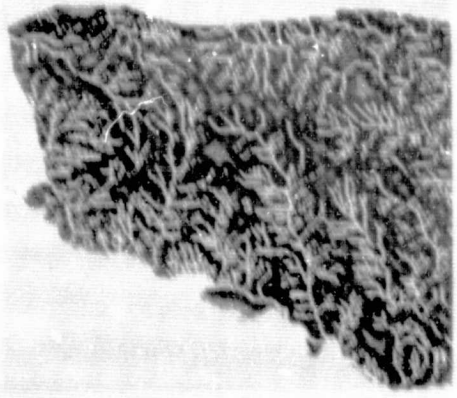

FIGURE 24. MAP OF MINIMUM DISTANCE TO DRAINAGE[3].

(SHORTEST DISTANCES IN BLACK)

A drainage map was interpreted from 75 of the low altitude black and white air photos of Dec. 1972. This map was, in turn, digitized to record the presence or absence of drainage in the 1 ha cellular data plane format. A minimum distance algorithm was applied to this binary data plane to compute the minimum distance from each empty cell not occupied by the drainage to the nearest cell through which the drainage passes.

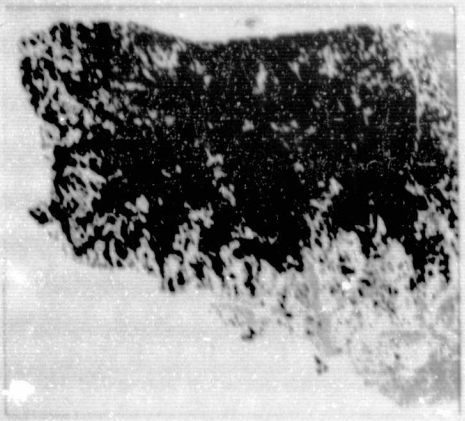

FIGURE 25. 2-VARIABLE CLASSIFICATION MAP*.

(GRID SAMPLED TRAINING SETS AND PROPORTIONAL APRIORI PROBABILITIES)

black ——→ *shifting cultivation and tea*
medium gray ——→ *irrigated rice*
light gray ——→ *hill evergreen forest*
white ——→ *4 other forest types*

The image was taken 27 Jan. 1973. The 8 cover types were classified using training sets derived from a 3 by 3 grid sample of the 1972 land cover data plane. The 2 variables analyzed were MSS-5 and MSS-7. The classification employed stepwise discriminant analysis with apriori probabilities directly proportional to the known occurrence of each land cover type in the site (i.e., proportional to the populations of these training sets).

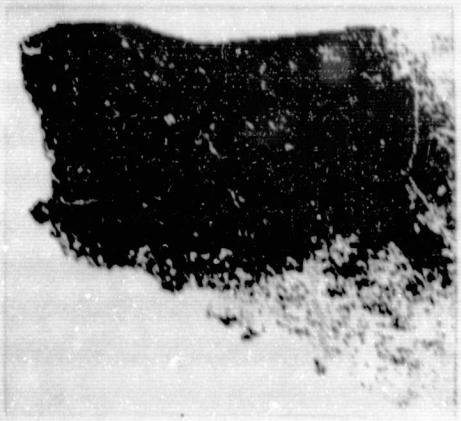

FIGURE 26. 4-VARIABLE CLASSIFICATION MAP*.

(GRID SAMPLED TRAINING SETS AND PROPORTIONAL APRIORI PROBABILITIES)

black ——→ *shifting cultivation and tea*
medium gray ——→ *irrigated rice*
light gray ——→ *hill evergreen forest*
white ——→ *4 other forest types*

This classification was identical to that noted in Figure 25 above except that it operated upon the 4 variables of MSS-4, 5, 6, and 7.

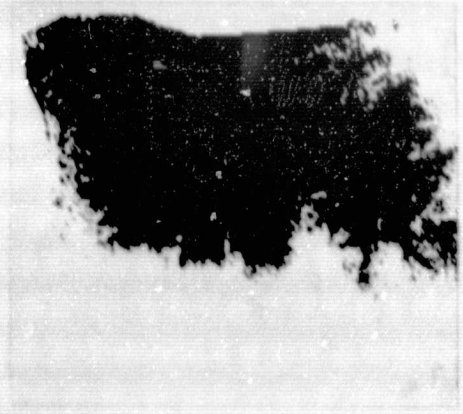

FIGURE 27. 8-VARIABLE CLASSIFICATION MAP*.

(GRID SAMPLED TRAINING SETS AND PROPORTIONAL APRIORI PROBABILITIES)

black ——→ *shifting cultivation and tea*
medium gray ——→ *irrigated rice*
light gray ——→ *hill evergreen forest*
white ——→ *4 other forest types*

This classification was identical to that noted in Figure 25 above except that it operated upon the 8 variables of MSS-4, 5, 6, and 7, slope, aspect, elevation, and distance to drainage.

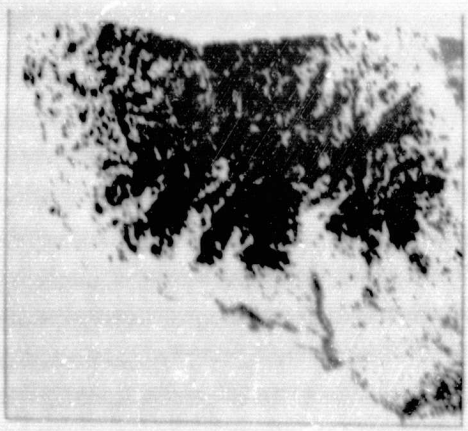

FIGURE 28. 8-VARIABLE CLASSIFICATION MAP*.

(GRID SAMPLED TRAINING SETS AND EQUAL APRIORI PROBABILITIES)

black ——→ *shifting cultivation and tea*
medium gray ——→ *irrigated rice*
light gray ——→ *hill evergreen forest*
white ——→ *4 other forest types*

This classification was identical to that noted in Figure 27 above except that it employed equal apriori probabilities of occurrence of each of the 8 cover types.

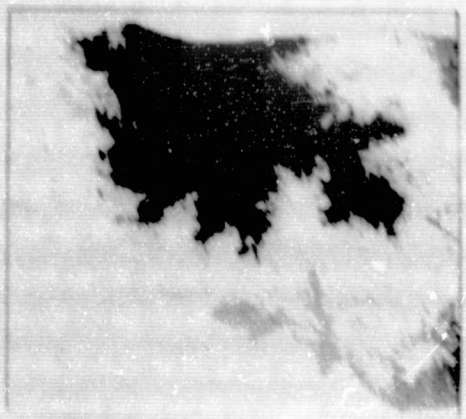

FIGURE 29. 8-VARIABLE CLASSIFICATION MAP*,
(RECTANGULAR TRAINING SETS AND PROPORTIONAL APRIORI PROBABILITIES)

black ——► shifting cultivation and tea
medium gray ——► irrigated rice
light gray ——► hill evergreen forest
white ——► 4 other forest types

The image was taken 27 Jan. 1973. The 8 cover types were classified using several rectangular training areas identified on the 1972 land cover data plane for each cover type sought. The 8 variables analyzed were MSS-4, 5, 6, and 7, slope, aspect, elevation, and distance to drainage. The classification employed stepwise discriminant analysis with apriori probabilities directly proportional to the known occurrence of each land cover type in the 1972 land cover type map.

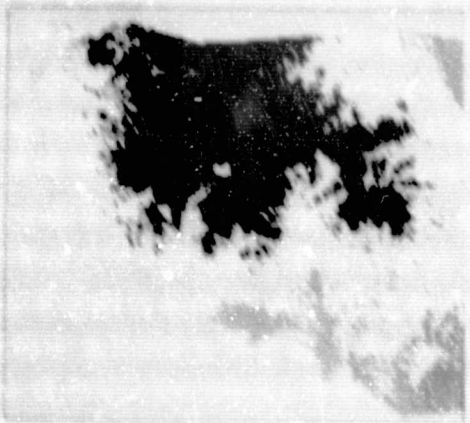

FIGURE 30. 8-VARIABLE CLASSIFICATION MAP*,
(RECTANGULAR TRAINING SETS AND EQUAL APRIORI PROBABILITIES)

black ——► shifting cultivation and tea
medium gray ——► irrigated rice
light gray ——► hill evergreen forest
white ——► 4 other forest types

This classification was identical to that noted in Figure 29 above except it employed equal apriori probability of occurrence of each of the 8 cover types.

FIGURE 31. 8-VARIABLE CLASSIFICATION MAP*,
(ASPECT TRAINING SETS AND PROPORTIONAL APRIORI PROBABILITIES)

black ——► shifting cultivation and tea
medium gray ——► irrigated rice
light gray ——► hill evergreen forest
white ——► 4 other forest types

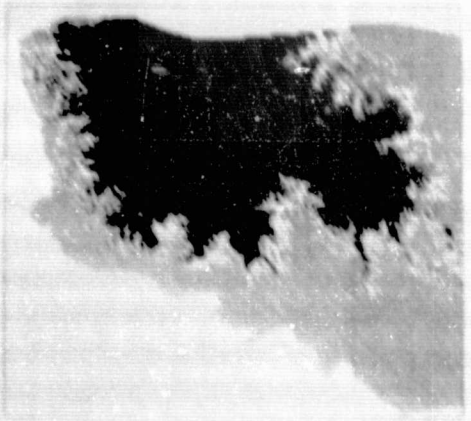

The image was taken 27 Jan. 1973. Each of the 8 cover types (less irrigated rice) was subdivided into 2 new classes representing generally east-tending and west-tending aspects so as to reduce the variance in each new class due to topographic induced radiance variation. These 14 new classes plus the 1 representing irrigated rice were classified using several rectangular areas to represent each class. The 8 variables analyzed were MSS-4, 5, 6, and 7, slope, aspect, elevation, and distance to drainage. The classification employed stepwise discriminant analysis with apriori probabilities directly proportional to the known occurrence of each land cover type in the 1972 land cover type map. After classification the two aspect classes representing each cover type were assigned the same identification to yield the original 8 cover types sought and displayed.

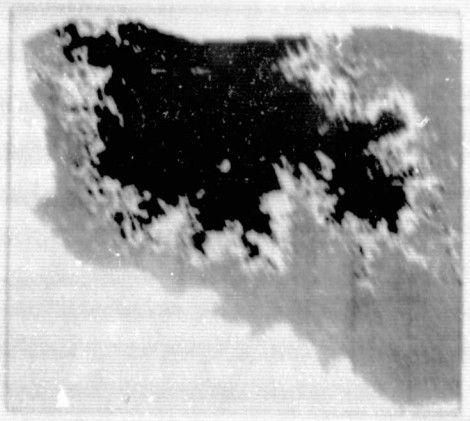

FIGURE 32. 8-VARIABLE CLASSIFICATION MAP*,
(ASPECT TRAINING SETS AND EQUAL APRIORI PROBABILITIES)

black ——► shifting cultivation and tea
medium gray ——► irrigated rice
light gray ——► hill evergreen forest
white ——► 4 other forest types

This classification was identical to that noted in Figure 31 above except it employed equal apriori probability of occurrence of each of the 15 cover types.

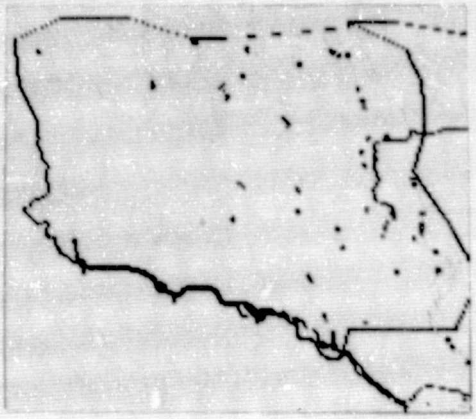

FIGURE 33. CULTURAL FEATURES MAP[3].

(SHOWS SITE BOUNDARY, ROADS AND TRAILS, TEMPORARY HUTS, AND PERMANENT HOUSING FEATURES)

A cultural features map was interpreted from the 75 low altitude black and white air photos of Dec. 1972. The map was, in turn, digitized to record the presence or absence of each of the cultural features in the 1 ha cellular data plane format. TEMPORARY HUTS represents individual brush shelters used for temporary or seasonal occupancy. PERMANENT HOUSING represents schools, field station, tea processing and storage areas, permanent dwellings, etc. ROADS AND TRAILS range anywhere from a heavily used footpath to improved dirt roads.

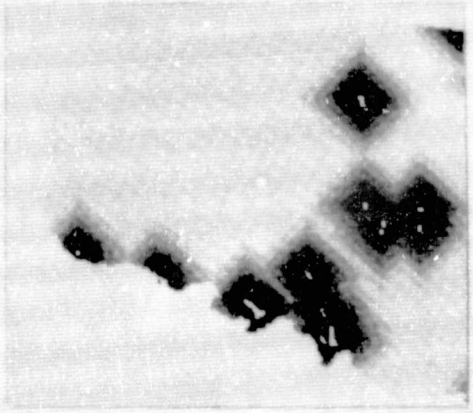

FIGURE 34. MAP OF MINIMUM DISTANCE TO PERMANENT HOUSING[4].

(SHORTEST DISTANCES IN BLACK)

A binary data plane was extracted from the cultural features data plane (Fig. 33) recording the presence or absence of areas of permanent housing in each 1 ha cell. The minimum distance algorithm was applied to compute the minimum distance from each empty cell not occupied by features of permanent housing to the nearest occupied cell. Diamond shaped patterns result from restriction of the minimum distance computation to combinations of N-S and E-W distances for reduced computation costs.

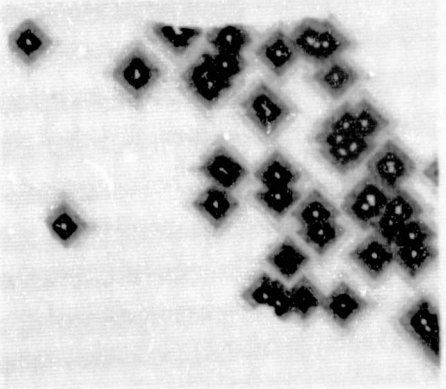

FIGURE 35. MAP OF MINIMUM DISTANCE TO TEMPORARY HUTS[4].

(SHORTEST DISTANCES IN BLACK)

A binary data plane was extracted from the cultural features data plane (Fig. 33) recording the presence or absence of temporary huts in each 1 ha cell. The minimum distance algorithm was applied to compute the minimum distance from each empty cell not occupied by a temporary hut to the nearest occupied cell. Diamond shaped patterns result from restriction of the minimum distance computation to combinations of N-S and E-W distances for reduced computation costs.

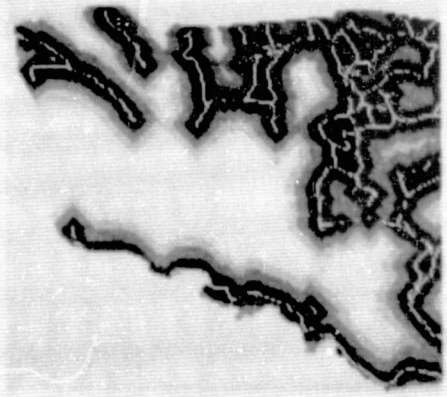

FIGURE 36. MAP OF MINIMUM DISTANCE TO ROADS AND TRAILS[4].

(SHORTEST DISTANCES IN BLACK)

A binary data plane was extracted from the cultural features data plane (Fig. 33) recording the presence or absence of a road or trail in each 1 ha cell. The minimum distance algorithm was applied to compute the minimum distance from each empty cell not occupied by a road or trail to the nearest occupied cell. Diamond shaped patterns result from restriction of the minimum distance computation to combinations of N-S and E-W distances for reduced computation costs.

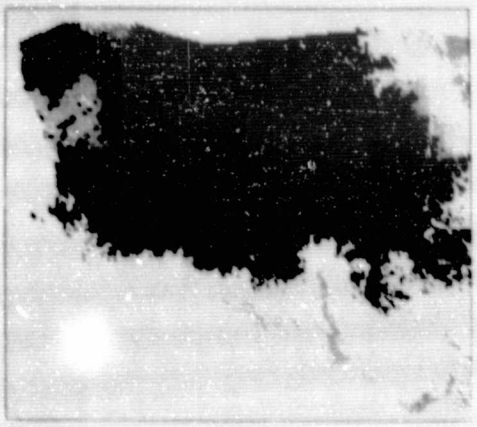

FIGURE 37. 11-VARIABLE CLASSIFICATION MAP*.

(GRID SAMPLED TRAINING SETS AND PROPORTIONAL APRIORI PROBABILITIES)

black ——→ shifting cultivation and tea
medium gray ——→ irrigated rice
light gray ——→ hill evergreen forest
white ——→ 4 other forest types

The 8 land cover types were classified using training sets derived from a 3 by 3 grid sample of the 1972 land cover data plane. The 11 variables analyzed were MSS-4, 5, 6, and 7, slope, aspect, elevation, distance to drainage, roads and trails, permanent housing, and temporary huts. The classification employed stepwise discriminant analysis with apriori probabilities directly proportional to the known occurrence of each land cover type in the site (i.e., proportional to the populations of these training sets).

FIGURE 38. 11-VARIABLE VERIFICATION MAP*.

(GRID SAMPLED TRAINING SETS AND PROPORTIONAL APRIORI PROBABILITIES - BLACK DENOTES POINTS CORRECTLY CLASSIFIED)

This display shows spatially those points which were correctly identified in the 11 variable classification map of Figure 37. Each and every 1 ha image cell has been classified into 1 of the 8 land cover classes and then checked against the corresponding 1 ha cell in the 1972 land cover data plane. When a 1 to 1 match occurred a black cell was displayed.

TABLE 1. COMPARISON OF VERIFICATION RESULTS FOR THE LANDSAT FOREST COVER CLASSIFICATIONS.

The numbers represent the percentage of the total number of the 29,290, 1 ha cells which were correctly classified into their respective cover type when checked against the 1972 land cover map. The second set of percentages in italics represent only those cells correctly classified into shifting cultivation. These italicized values for shifting cultivation fluctuate widely as the various classification approaches were optimized to achieve the best overall accuracy for all 8 land covers and not optimized for this specific cover type.

2 variables used = MSS-5 and 7,
4 variables used = those above plus MSS-4 and 6,
8 variables used = those above plus topographic slope, aspect, elevation, and distance to drainage,
11 variables used = those above plus distance to roads and trails, permanent housing, and temporary housing.

VARIABLES USED	TYPE OF TRAINING SETS							
	RECTANGULAR		ASPECT		GRID	
	Equal	Proportional	Equal	Proportional	Equal	Proportional
2	26.0 *15.8*	43.6 *67.6*	19.0 *14.1*	41.4 *61.9*	22.1 *13.6*	41.7 *66.7*
4	26.2 *16.6*	44.5 *64.8*	33.6 *87.9*	39.0 *99.0*	28.0 *27.4*	48.8 *83.3*
8	33.4 *34.9*	43.9 *47.4*	22.6 *34.7*	29.6 *54.4*	32.9 *35.6*	52.2 *72.7*
11	n.c. *n.c.*	46.1 *46.4*	n.c. *n.c.*	n.c. *n.c.*	38.1 *37.8*	55.4 *76.7*

n.c. = not computed